

Transverse mode selection in a monolithic microchip laser

Darryl Naidoo^{a,b}, Thomas Godin^c, Michael Fromager^c, Emmanuel Cagniot^c, Nicolas Passilly^d, Andrew Forbes^{a,b} and Kamel Aït-Ameur^{c1}

^a:CSIR National Laser Centre, P. O. Box 395, Pretoria 0001, South Africa

^b:School of Physics, University of KwaZulu-Natal, Private Bag X54001, Durban 4000, South Africa

^c:Centre de Recherche sur les Ions, les Matériaux et la Photonique, UMR 6252, CEA-CNRS-ENSICAEN et Université de Caen, ENSICAEN, 6 Boulevard Maréchal Juin, F-14050 Caen, France.

^d:Institut FEMTO-ST, UMR 6174, CNRS-ENSMM et Université Technologique de Belfort-Monbéliard, 32 Avenue de l'Observatoire, F-25044 Besançon cedex, France

We outline an approach to mode selection in a microchip laser through judicious shaping of the pump light to create a high modal overlap with the desired mode. We demonstrate the principle by creating a donut-shaped pump profile in the focal plane of a converging lens, and use this profile to longitudinally pump a monolithic microchip laser where the output is a Laguerre-Gaussian mode of radial index $p=0$ and azimuthal index $l=1$ (LG_{01}), or vortex beam, of power ~ 12 mW with a slope efficiency of 17%. This approach of diffractive pump shaping in the Fourier domain is advantageous as it allows for high pump intensity even with low pumping powers, thus ensuring sufficient gain is achieved for laser oscillation.

OCIS codes: 140.3300, 140.3945, 140.3570, 140.5560.

Key words: Pump shaping, microchip laser, vortex beam, higher order modes

¹ Corresponding author: Kamel Aït-Ameur; tel: + 02 31 45 25 73; fax: + 02 31 45 25 57; email: kamel.aitameur@ensicaen.fr

1. Introduction

High brightness lasers, particular of the solid-state design, are of considerable interest in industry, the military and academia, and have been exploited in applications such as remote sensing, ultrafast spectroscopy, laser precision materials processing and laser weapons applications [1]. In general the output mode of the laser is not ideally suited to the application at hand; this deficiency is overcome by either shaping the laser beam external to the cavity, or inserting beam shaping elements intra-cavity in order to force the laser to oscillate on the desired mode [2]. When the desired beam is one of the eigenmodes of the Laguerre-Gauss basis (denoted by LG_{pl} in the rest of this paper, where p is the radial order and l the azimuthal order), the problem of selecting a desired higher order mode is non-trivial [3], with very little attention paid to this subject in the literature. Indeed, selecting modes of this family is almost always accomplished by insertion of intra-cavity components such as amplitude mask [4], phase mask [5] or a lens with strong spherical aberration [4]. The selection of a given single high-order transverse mode is as usual based on amplitude differences between the modes (e.g., the physical size). But is it possible to select such modes without the aid of intra-cavity elements? To date this question has not been sufficiently addressed in the literature, with very few reported attempts [7,8,9]. Of particular interest, and the subject of this paper, is the selection of LG_{0l} modes, otherwise known as vortex beams or “donut” modes, of pure modal quality (i.e., not superpositions of such beams [7, 9]), which we demonstrate with the aid of a microchip laser cavity. Such beams have found application in such diverse topics as the guiding of ultra-cold atomic beams [10, 11], trapping of small particles [12, 13], improvement of confocal microscope performance [14], LIDAR applications [15], and quantum information processing [16]. Such fields are consequently highly topical, and of much interest to the community at large. They are routinely generated external to the cavity [17], and may be generated intra-cavity with the aid of special mode selecting elements [18].

In this paper we extend the previous ideas [7-9] on pump shaping and outline an approach to selecting such modes based on diffractive shaping of the pump beam. The idea is simply that by shaping the pump, we may create arbitrarily good overlap between the pump and the desired mode,

and thus force the laser oscillation on a transverse mode of higher order rather than the usual (low order) Gaussian mode. One may thus think of the pump beam intensity profile as a parameter of transverse mode control not often exploited in laser resonator experiments. We will demonstrate this principle on a diode-pumped monolithic microchip laser, where the pump beam has been suitably shaped (in intensity profile). Microchip lasers have interesting properties in that, firstly, the cavity length is remarkably short such that only a single longitudinal mode is achieved thus ensuring single-frequency output, and secondly, due to the flat-flat configuration and end pumping of the gain, a Gaussian mode is strongly favoured in oscillation [19]. Without any intra-cavity elements (which are by definition forbidden in such lasers), we will show that such a laser can be made to oscillate on a mode other than the Gaussian, and we illustrate this for the case of a dark hollow beam known as *donut mode*.

2. The donut mode

We are interested to force the microchip laser oscillation on an eigenmode having the shape of a dark hollow beam. Such laser beams are interesting when they are structurally stable in the sense that they propagate without changing shape, when radial scaling is omitted. The donut mode can be a pure Laguerre-Gauss mode or a superposition of Hermite-Gauss modes. Before to proceed let us recall the salient equations governing such modes.

The first family of modes we consider is the Laguerre-Gaussian modes which are solutions of the wave equation in circular symmetry. These eigenmodes are denoted LG_{pl} where the transverse mode indices p and l correspond to the radial order and azimuthal order, respectively. The electric field distributions of these eigenmodes read as [20]

$$\begin{aligned}
 u_{p,l} = & \sqrt{\frac{2p!}{\pi(p+|l|)!}} \frac{1}{w(z)} \left[\frac{\sqrt{2}r}{w(z)} \right]^{|l|} L_p^{|l|} \left[\frac{2r^2}{w(z)^2} \right] \\
 & \times \exp \left[\frac{-r^2}{w(z)^2} - \frac{ikr^2}{2R(z)} \right] \exp \left[-i(2p+|l|+1) \arctan \left(\frac{z}{z_R} \right) \right] \exp(il\phi)
 \end{aligned} \tag{1}$$

where z_R is the Gaussian Rayleigh range, $w(z)$ is the Gaussian beam width at some propagation position z and $L_p^{|l|}$ is the generalised Laguerre polynomial. All other terms have their usual meaning. The lowest order mode, LG_{00} , corresponds to the well know Gaussian beam, while higher radial (p) and azimuthal (l) orders also exist as possible solutions. Generally speaking, such higher order modes exhibit larger spatial distributions, higher divergence, and in an apertured laser cavity, larger losses [21], but by inserting a phase or amplitude mask inside the laser cavity it is possible to force the laser oscillation on a single high order transverse mode [3-5]. By use of the second order intensity moments one can derive a simple expression for the laser beam quality factor for a Laguerre-Gaussian mode LG_{pl} as

$$M^2 = 2p + |l| + 1. \quad (2)$$

Equations (1) and (2) uniquely define the field at all planes during propagation. It can be shown also that apart from a scaling factor, Equation (1) is the Fourier transform of itself, thus the shape of such modes is propagation invariant, but not scale invariant.

For $p=0$ and $l \geq 1$ the LG_{pl} modes have an intensity profile that is radially symmetric, with zero intensity in the centre. It looks like a donut when this mode is projected on a screen or a CCD camera. The particularity of LG_{0l} modes lies in their phase structure which winds as a function of angle ϕ . In a transverse plane, the phase smoothly advances with angle ϕ , counter-clockwise for $l>0$ and clockwise for $l<0$. In fact the modes $LG_{0,-l}$ and $LG_{0,l}$ constitute an optical vortex. It is worthwhile to recall that an optical vortex is a singularity point where the amplitude vanishes and the phase is undetermined. The phase circulation around the singularity point is an integer multiple of 2π . It results that such a beam possesses an orbital angular momentum.

Another way to produce a donut eigenmode is to combine coherently linearly polarised Hermite-Gauss TEM_{01} and TEM_{10} modes. There are four ways to combine TEM_{01} and TEM_{10} modes resulting in different polarisation states of the resulting sum mode usually denoted TEM_{01^*} . This has

been described by H. Kogelnik and T.Li [22], and the state of polarisation of the TEM_{01^*} is inhomogeneous and can be radial, azimuthal or hybrid. It is worthwhile to recall that the well known linearly polarised and circular polarised laser beams are characterised by a state of polarisation which does not depend upon the position in the cross-section of the beam. These types of polarisation are referred as homogeneous polarisations. In contrast, an inhomogeneous polarised beam has a state of polarisation varying over the cross-section. This property makes easy the identification of an inhomogeneous polarisation by placing a linear polariser since the emerging intensity pattern is made-up of two-lobed irradiance pattern that rotates with the polariser axis [23]. From the second order intensity moments one can obtain the laser beam quality factor for a Hermite-Gaussian mode HG_{mn} as

$$M_x^2 = (2m + 1) \quad \text{and} \quad M_y^2 = (2n + 1). \quad (3)$$

The coherent combining of TEM_{01} and TEM_{10} modes leading to the hybrid TEM_{01^*} mode is characterised by a beam quality factor $M^2 = 2$ [24]. As a consequence, the measurement of the beam quality factor of a donut eigenmode does not allow to distinguish between a Laguerre-Gauss mode ($p=0$ and $l = \pm 1$) and a TEM_{01^*} mode. However, as shown above the polarisation properties of the two kinds of donut mode will enable us to prove the nature of the donut mode involved in the experiment.

3. Resonator concept and experimental set-up

A microchip laser in its simplest form consists of a thin slice of solid-state gain material polished flat and parallel on two sides and where the cavity mirrors, which are flat, are dielectrically deposited onto the surfaces. A flat-flat cavity has eigenmodes that are plane waves for a passive system, but for microchip lasers the thermally induced refractive index change, due to heat deposited by the incident pump beam, results in a waveguide. The deposited heat also assists in thermal expansion of the gain medium, which can result in end-face curvature; this allows the laser to sustain a stable oscillation in the form of a single-mode waveguide [19]. Indeed, monolithic microchip lasers have the Gaussian

beam as the eigenmode due to index guiding (associated with thermal effects) and gain guiding (connected to a Gaussian pump profile) even several times over the threshold.

We consider a monolithic microchip that is end-pumped by a single mode fibre coupled diode laser (Gaussian beam) emitting at a wavelength of 808 nm with a maximum power of 160 mW. A schematic of the set-up is shown in Fig. 1. The microchip consists of a thin slice (5 x 5 x 0.5 mm) of Nd:YVO₄ polished flat and parallel on opposing sides, and with dielectric mirrors deposited directly onto the polished surfaces to act as the cavity mirrors. As the mirrors are deposited directly onto the crystal, the cavity length is very short, thus ensuring single-frequency behaviour. Intra-cavity elements are thus not permissible and consequently an intra-cavity approach in the generation of a LG₀₁ beam by inserting a phase or amplitude mask is not possible. The only parameter that can be modified in a monolithic microchip laser for transverse mode selection, generally speaking, is the pump beam: its size, shape and power.

We reshape our Gaussian pump beam by the use of a diffractive optical element in the form of a π -plate (see Fig. 2a), which introduced a π phase shift in the central region of an incident collimated Gaussian beam. By adjusting the ratio ($\Delta = b/w$) of the incident Gaussian width (w) to the π -plate radius (b), various beam shapes could be produced in the far field [25], which was realised at the focal plane of a lens positioned just after the π -plate. Relevant to this study, it was possible to achieve a donut-shaped profile (see Fig. 2b), for Δ between 0.7 – 0.9. Our hypothesis is that by pumping the microchip with a donut-shaped intensity profile, so that the overlap integral between the pump and the desired mode is high, the desired mode will oscillate preferentially. This may be considered as indirect shaping of the gain.

The Gaussian pump was telescoped to a width of ~1 mm, resulting in a ratio $\Delta = 0.72$. This produced a good quality donut shaped beam (see Fig. 3a) of second moment radius ~50 μ m at the focal plane of a lens ($f = 100$ mm). The size of the shaped beam could be controlled through the choice of the focal length of the lens, without changing the intensity profile of the shaped light. Our pump beam at the focal plane was not shape invariant during propagation; however, the effective Rayleigh range of the beam (defined as the distance over which the beam shape did not change appreciably) was ~3 mm, which is 6 times greater than the thickness of the crystal (0.5 mm). This

ensured that the pump shape could be considered invariant over the length of the cavity. The Gaussian pump (see Fig. 3b) without any beam shaping element focussed (using the same lens) to a radius of $\sim 17 \mu\text{m}$ with a Rayleigh range of $\sim 0.6 \text{ mm}$. The output beam from the laser was analysed using a CCD camera (Cohu 4812) and the beam quality factor (M^2) measured by use of a beam diagnostic tool (Spiricon M^2 -200 equipped with a Cohu 4812 CCD camera).

4. Results and Discussion

With a donut shaped pump beam (Fig. 3a) the microchip laser oscillated in a donut transverse mode, as shown in Fig. 3c, while without the diffractive optical element (i.e., no pump beam shaping) the microchip laser reverted to the standard Gaussian output mode (see Fig. 3d). The donut output beam had a maximum power of $\sim 12 \text{ mW}$, with a slope efficiency of 17% (see Fig. 4a). The propagation of the resulting mode was measured, and depicted in Fig. 4b, and has been identified as a Laguerre-Gauss mode LG_{pl} with $p=0$ and $l=1$ as it will be discussed in the following. The intensity profile of the output beam remained the same shape during propagation to the far field (shown in the inset of Fig. 4b), with measured M^2 values in the two principal axes of $M_x^2 = 1.94$ and $M_y^2 = 1.95$, in excellent agreement with the expected theoretical value of 2 (for both axes) for a donut mode, as shown in Section 2. The excellent symmetry maintaining properties of such a cavity account for the emergence of the azimuthal mode as compared to odd or even modes observed by others in similar lasers [7,9]. Without pump beam shaping the microchip laser reverted to a good quality Gaussian output mode ($M_x^2 = 1.04$ and $M_y^2 = 1.03$) with a maximum power of $\sim 30 \text{ mW}$ and with a slope efficiency of 26%.

From the measured propagation, it is possible to predict the beam size at the output coupler assuming a mode of the type given by Eq. (1). The predicted intensity together with the measured intensity is shown in Fig. 5a, and clearly there is excellent agreement between the two. Since Eq. (1) defines the mode everywhere in space, a match to the propagation (as evident from Figs. 4b and 5a) is confirmation of the spatial structure of the field. It is instructive to compare the propagation of the output laser mode @1064nm to that of the pump. The pump beam is also a hollow mode, but only at one plane: in fact the propagation from the flat-top mode to the hollow mode follows a trend very

similar to that shown from the top cross-section of Fig. 2b moving to the bottom cross-section [25]. This differs from the measured propagation of the laser mode, which is a hollow beam everywhere. There is the remote possibility that despite the symmetry of the pump beam, the microchip laser may be oscillating in a coherent superposition of Hermite-Gaussian modes, so that the central intensity null is not due to the azimuthal phase variation of the $l = 1$ Laguerre-Gaussian mode, but rather due to a singularity associated with an inhomogeneous polarised mode. The output laser mode was passed through a polariser that was rotated through all angles, and the intensity and mode structure monitored. It was observed that the transmission was constant for all angles of the polariser, and that the mode structure remained invariant, with the results for the vertical and horizontal alignments of the polariser shown in Fig. 5b and 5c respectively. This negates the possibility of, for example, a radially or azimuthally polarised mode due to a superposition field, which may also result in a central intensity null. To summarise: the laser beam quality factor is consistent with a LG_{01} mode in the Laguerre-Gaussian mode basis, the propagation is consistent with this mode and with none other, and finally other remote possibilities of superpositions that generate intensity nulls such as radially polarised beams have also been eliminated. Thus we can say with confidence that we have verified single mode lasing in a LG_{01} mode. As pointed out in the introduction, such modes carry orbital angular momentum; the “vortex” or phase singularity that gives rise to this is a direct result of the spatial structure of the field. We have measured this spatial structure by considering the propagation of the field. It is also possible to visualise the phase singularity by interference with a reference wave without a vortex, resulting in a fork-like discontinuity in the interference pattern; such techniques are routinely used when vortex beams are created external to the cavity [26]. However, when the vortex beam is created intra-cavity, no plane wave or Gaussian reference field exists with which to execute such an experiment. We suggest that it may be possible to visualise the vortex by executing an inner product of the laser mode with an azimuthally varying phase function, which may be generated as a diffractive optical element or as a digital hologram on a spatial light modulator.

The process of exciting the higher order mode by shaping the pump light is also influenced by the pump beam size, as the overlap integral between the desired mode and the pump mode can be increased or decreased depending on the ratio of the pump size to the mode size. A plot of the two

pumps, with corresponding output beams, is shown in Fig. 6, where the overlap of the modes with the pumps is evident. When the pump size was decreased by decreasing the focal length of the Fourier transforming lens (to $f = 75$ mm), a Gaussian shaped output was produced. However, when the pump size was increased by use of a longer focal length lens ($f = 125$ mm), the LG_{01} mode was again preferred, but with less efficiency (maximum power of ~ 11 mW with a slope efficiency of 15%). A marginal decrease in modal quality was also noted, with the beam quality factor measured to be $M_x^2 = 1.88$ and $M_y^2 = 1.96$. However, the scaling was not sufficient to generate even higher order LG_{0l} modes.

The lower output power and slope efficiency of the LG_{01} (donut) mode as compared to the LG_{00} (Gaussian) mode in the case of a shaped pump and Gaussian pump respectively can be understood if one considers that the reshaping of the pump is accompanied by an increase in the focal spot size of the pump in comparison with that of the focused Gaussian pump beam. The ratio of these two radial quantities is equal to the M^2 factor of the donut-shaped pump, which is known [25] to be roughly 4. Thus the pumping intensity is reduced when the pump beam is reshaped, and this is consistent with the observation of a lower output power (~ 12 mW) as compared to the Gaussian output case (~ 30 mW) when the pump beam is Gaussian. However, the factor of reduction is not equivalent to 4 because the energy is removed from the centre toward the periphery inside a ring, as evident in Fig. 6.

There are several advantages to using a scheme where the beam shaping element is designed to produce the desired mode in the far field. Most notable (using the example of the π -plate) is the fact that the donut-shaped pump is obtained at the focal plane of a converging lens, thus allowing for high intensity within the crystal even with low pumping powers: sufficient gain is achieved for obtaining laser oscillation. In principle any diffractive optical element (or equivalent beam shaping system) could replace the π -plate as the shaping step in the process, while with suitable coatings and design considerations, such beam shaping elements can be very close to 100% efficient.

We end this study by pointing out that amplitude diffraction can also transform a Gaussian beam into a donut shaped beam: if one passes a collimated Gaussian (pump) beam through a circular

aperture, then one observes [27] in the near-field region a donut intensity profile, where the dip in the centre of the donut reduces as the aperture is closed (i.e., it is scalable). A gain medium may be set in this plane, and Bisson *et al* [8] have experimentally implemented this approach to pump a Nd:YAG laser with a donut-shaped pump. However, two important drawbacks were noted: the laser only operated at high pump powers; this can be explained by the fact that the donut pump is only available in the near-field of the aperture where the pump sizes are relatively large, and not at the focal plane of a lens where the pump size can be very small. The second drawback was the severe attenuation due to the hard-aperture clipping, resulting in low conversion of the Gaussian to the hollow beam pattern. Indeed, from pump pulse energies of hundreds of mJ the output mode from the Nd:YAG laser consisted of pulses having energy of only some tens of μJ : a slope efficiency of $\sim 0.01\%$, or approximately three orders of magnitude lower than the results reported here. The power scaling of our technique requires only that the input pump beam to be shaped exhibits some coherence, for example, high power fibre lasers or fibre delivered diode pumps. Indeed, one can imagine this pumping scheme as simply adding an adequate diffractive optical element to the pump delivery optics without any other changes to the set-up, as most pump delivery schemes already make use of a lens to focus the pump. Thus power scaling limitations due to material damage and thermal management will be the same in this scheme. The advantage of this scheme is much improved slope efficiency for the generation of higher order modes as compared to amplitude based techniques for such mode selection [8].

In summary, this study demonstrates that stable generation of a pure Laguerre-Gauss mode LG_{pl} with $p=0$ and $l=1$ is possible with a monolithic microchip thanks a reshaping of the pump beam by using a simple binary diffractive optical element referred as π -plate. The LG_{01} mode not only behaves as a donut-like pattern but is also accompanied by the phenomenon of optical vortices rendering possible the transfer of angular momentum between light and matter very useful for trapping and rotating of micro and nano-particles. It is important to note that the single frequency behaviour of the monolithic microchip is well adapted to cold atoms guiding since its oscillation frequency can be easily adjusted by controlling the temperature of the laser crystal. Finally, the apparatus based on the use of a

monolithic microchip for generating a vortex beam could present the advantage to be more easily compacted and stable than a mode converter involving interferometric techniques [28,29].

5. Conclusion

We have successfully demonstrated mode control in a microchip laser through appropriate shaping of the pump light, thus indirectly shaping the gain. In particular, we have used this concept to optimising the gain medium of a microchip laser with a donut-shaped pump profile, and shown that we can achieve a LG_{01} (vortex beam) as the fundamental eigenmode of the cavity. The shaping of the Gaussian pump beam was achieved by the use of a π -plate where it introduced a π phase shift in the central region of an incident collimated Gaussian beam. This method of pump shaping is advantageous as the donut-shaped pump is obtained in the focal plane of a converging lens which allows for high intensity and with low pumping powers, and in general this principle of pump shaping in order to maximise the overlap between the pump and the desired mode should allow for arbitrary modes to be generated from such cavities without the need for intra-cavity mode selecting elements. In the case of microchip lasers, where intra-cavity shaping elements are not permissible, this approach opens a more effective method for complex mode generation from microchip lasers, and thus tailoring of the lasers to new applications.

ACKNOWLEDGEMENTS

The authors acknowledge the support of the Conseil Régional Basse Normandie, and the join research grant PROTEA 07 F/45/SA under the France South Africa scientific cooperation agreement.

References

- [1] R. L. Byer, "Diode Pumped Solid State Lasers," CLEO Pacific Rim, (2009).
- [2] J. R. Leger, D. Chen and Z. Wang, "Diffractive optical element for mode shaping of a Nd:YAG laser," *Opt. Lett.* **19** (1994) 108-110.
- [3] A. A. Ishaaya, N. Davidson, G. Machavariani, E. Hasman and A. A. Friesem, "Efficient selection of High-order Laguerre-Gaussian modes in a Q-switched Nd:YAG laser," *IEEE J. Quant. Elec.* **39** (2003) 74-82.
- [4] A. Hasnaoui, K. Aït-Ameur, "Properties of a laser cavity containing an absorbing ring", *Appl. Opt.* **49** (2010) 4034-4043.
- [5] E. Cagniot, M. Fromager, T. Godin, N. Passilly, M. Brunel, K. Aït-Ameur, "A variant of the method of Fox&Li dedicated to intracavity laser beam shaping", *JOSA A* **28**, 489-495 (2011).
- [6] M. Thirugnanasambandam, Y. Senatski, A. Shirakawa, K. Ueda, Multi-ring modes generation in Yb:YAG ceramic laser", *Opt. Mat.* **33** (2010) 675-678.
- [7] Y. F. Chen and Y. P. Lan, "Laguerre-Gaussian modes in a double-end-pumped microchip laser: superposition and competition," *J. Opt. B: Quantum Semiclass. Opt.* **3**, 146-151 (2001).
- [8] J-F. Bisson, A. Shirakawa, Y. Sato, Y. Senatsky and K-I. Ueda, "Near-field diffractive optical pumping of a laser medium," *Opt. Rev.* **11** (2004) 353-357.
- [9] Y. F. Chen, Y. P. Lan and S. C. Wang, "Generation of Laguerre-Gaussian modes in fiber-coupled laser diode end-pumped lasers," *Appl. Phys. B* **72** (2001) 167-170.
- [10] Z. Wang, Y. Dong and Q. Lin, "Atomic trapping and guiding by quasi-dark hollow beam," *J. Opt A: Pure Appl. Opt.* **7** (2005) 147-153.
- [11] F. K. Fatemi and M. Bashkansky, "Cold atom guidance using a binary spatial light modulator," *Opt Express* **14** (2006) 1368-1375.
- [12] A. Jesacher, S. Fürhapter, S. Bernet and M. Ritsch-Marte, "Size selective trapping with optical cogwheel tweezers." *Opt. Express* **12** (2004) 4129-4135.

- [13] M. Gu, D. Morrish and P. C. Ke, “Enhancement of transverse trapping efficiency for a metallic particle using an obstructed laser beam,” *Appl. Phys. Lett.* **77** (2000) 34-36.
- [14] W. Zhao, J. Tan and L. Qui, “Improvement of confocal microscope performance by shaped annular beam and heterodyne confocal techniques,” *Optik* **116** (2005) 111-117.
- [15] T. Shiina, K. Yoshida, M. Ito and Y. Okamura, “Long-range propagation of annular beam for lidar application,” *Opt. Comm.* **279** (2007) 159-167.
- [16] J. B. Götte, K. O’Holleran, D. Preece, F. Flossmann, S. Franke-Arnold, S. M. Barnett and M. J. Padgett, “Light beams with fractional orbital angular momentum and their vortex structure,” *Opt. Exp.* **16** (2008) 993-1006.
- [17] S. A. Kennedy, M. J. Szabo, H. Teslow, J. Z. Porterfield and E. R. I. Abraham, “Creation of Laguerre-Gaussian modes using diffractive optics,” *Phys. Rev. A.* **66** (2002) 043801-1-043801-5.
- [18] Y. Senatsky, J-F. Bisson, A. Shelobolin, A. Shirakawa and K. Ueda, “Circular modes selection in Yb:YAG laser using an intracavity lens with spherical aberration,” *Laser Phys.* **19**(2009) 911-918.
- [19] J. J. Zayhowski, “Microchip Lasers,” *Optical Materials* **11** (1999) 255-267.
- [20] A. Vaziri, G. Weihs and A. Zeilinger, “Superpositions of the orbital angular momentum for applications in quantum experiments,” *J. Opt. B: Quantum Semiclass. Opt.* **4** (2002) S47 – S51.
- [21] N. Hodgson and H. Weber, *Laser Resonators and Beam Propagation* (Springer, 2005).
- [22] H. Kogelnik and T. Li, “Laser beams and resonator”, *Appl. Opt.* **5** (1966) 1550-1567.
- [23] D.J. Armstrong, M.C. Phillips, A.V. Smith, “Generation of radially polarised beams with an image-rotating resonator”, *Appl. Opt.* **42** (2003) 3550-3554.
- [24] D.R. Hall and P.E. Jackson, “The Physics and Technology of Laser Resonators”, chap. 9 , Institut Of Physics Ltd (1989).
- [25] R. de Saint Denis, N. Passilly, M. Laroche, T. Mohammed-Brahim and K. Ait-Ameur, “Beam-shaping longitudinal range of a binary diffractive element,” *Appl. Opt.* **45** (2006) 8136-8141.

- [26] R. Vasilyeu, A. Dudley, N. Khilo and A. Forbes, “Generating superpositions of higher-order Bessel beams,” *Opt. Express* **17** (2009) 23389-23395.
- [27] R. Bourouis, K. Aït-Ameur and H. Ladjouze, “Optimization of the Gaussian beam flattening using a phase-plate,” *J. Mod. Optics* **44** (1997) 1417-1427.
- [28] S.M. Iftikar, “A tunable doughnut laser beam for cold-atom experiments”, *J. Opt. B: Quantum Semiclass. Opt.* **5** (2003) 40-43.
- [29] S. Chu, K. Otsuka, “Doughnut-like beam generation of Laguerre-Gauss mode with extremely high mode purity”, *Opt. Commun.* **281** (2008) 1647-1653.

Figure Captions

Figure 1: Schematic of the experimental setup for optically pumping a microchip laser with a donut-shaped pump intensity profile. The beam shaping element could be removed to revert back to the Gaussian pump scenario.

Figure 2: (a) Schematic of a π -plate where a π phase shift is introduced in the central region of an incident collimated Gaussian beam, (b) Intensity distributions displaying the phase transformation of a collimated Gaussian beam incident on a π -plate at the focal plane of a focusing lens [18].

Figure 3: Intensity profiles for (a) donut-shaped pump, (b) Gaussian pump, (c) output far-field intensity of a microchip laser oscillating in a LG_{01} (donut) eigenmode, and (d) Gaussian output when pumped with a Gaussian beam.

Figure 4: (a) Slope efficiencies of a Gaussian and LG_{01} output with the Gaussian and donut shaped pump profiles respectively; (b) Free space propagation of the LG_{01} beam (in the two principal axes) from which the beam quality factor (M^2) could be inferred (and similarly for the Gaussian beam). The inset in (b) shows the far-field image of the LG_{01} eigenmode.

Figure 5: (a) Comparison of the intensity profiles calculated LG_{01} mode at the output coupler and the measured intensity, showing good agreement. The intensity is invariant under rotation of polarisation: (b) after passing through a vertically aligned polariser and (c) a horizontally aligned polariser.

Figure 6: Intensity profiles of the Gaussian and LG_{01} modes for the correspondingly shaped pump beam, for the $f = 100$ mm case. The overlap between the modes, and well as the distribution of energy, is evident.

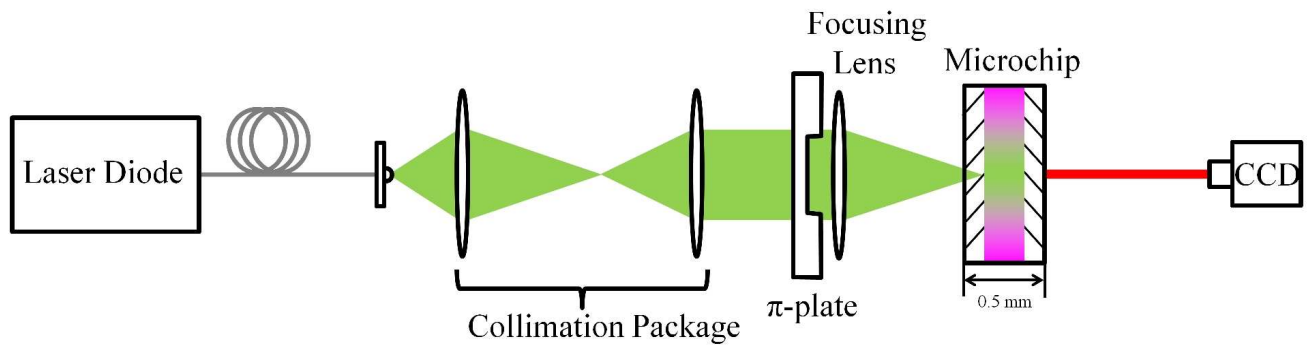


Figure 1: Schematic of the experimental setup for optically pumping a microchip laser with a donut-shaped pump intensity profile. The beam shaping element could be removed to revert back to the Gaussian pump scenario.

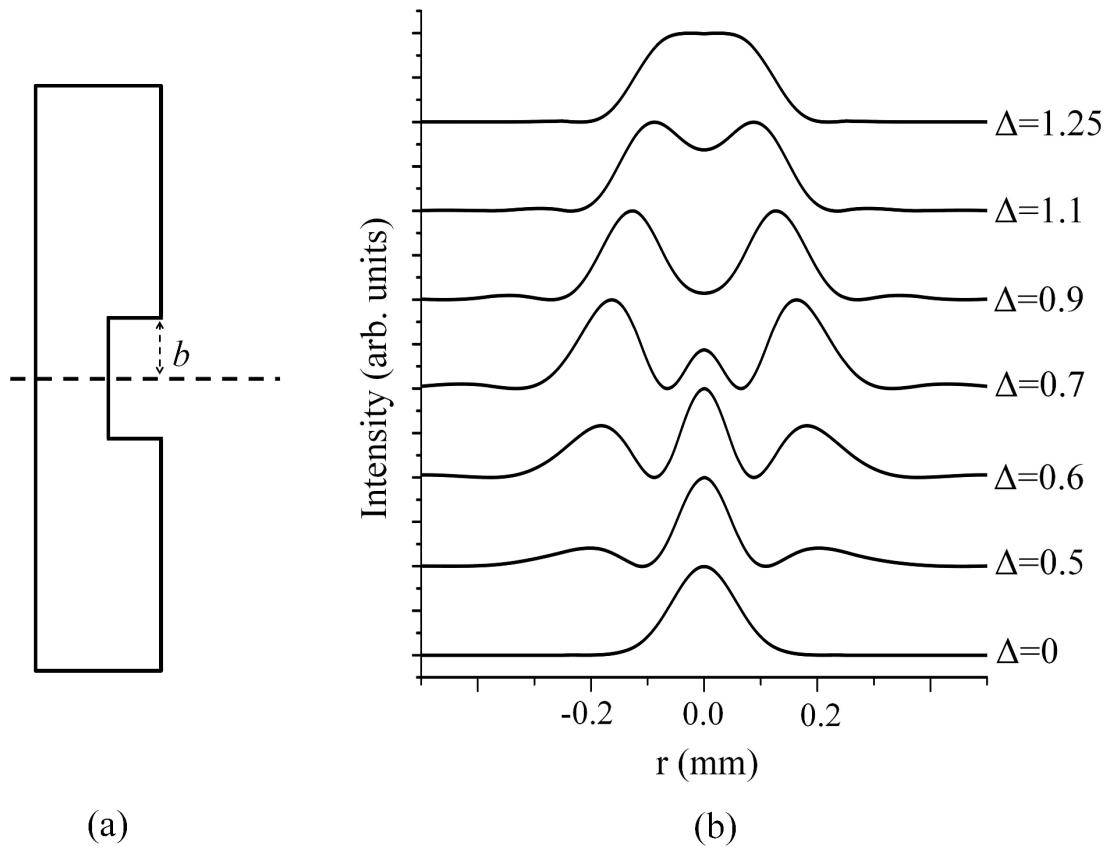


Figure 2: (a) Schematic of a π -plate where a π phase shift is introduced in the central region of an incident collimated Gaussian beam, (b) Intensity distributions displaying the phase transformation of a collimated Gaussian beam incident on a π -plate at the focal plane of a focusing lens [18].

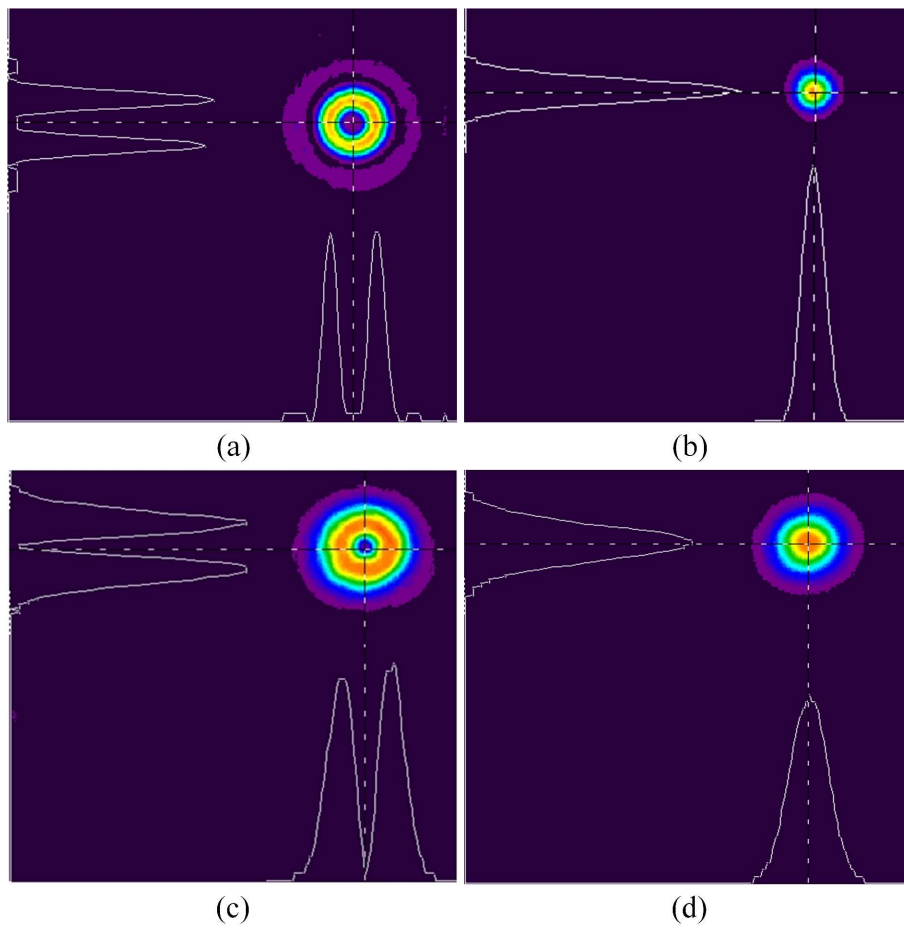


Figure 3: Intensity profiles for (a) donut-shaped pump, (b) Gaussian pump, (c) output far-field intensity of a microchip laser oscillating in a LG_{01} (donut) eigenmode, and (d) Gaussian output when pumped with a Gaussian beam.

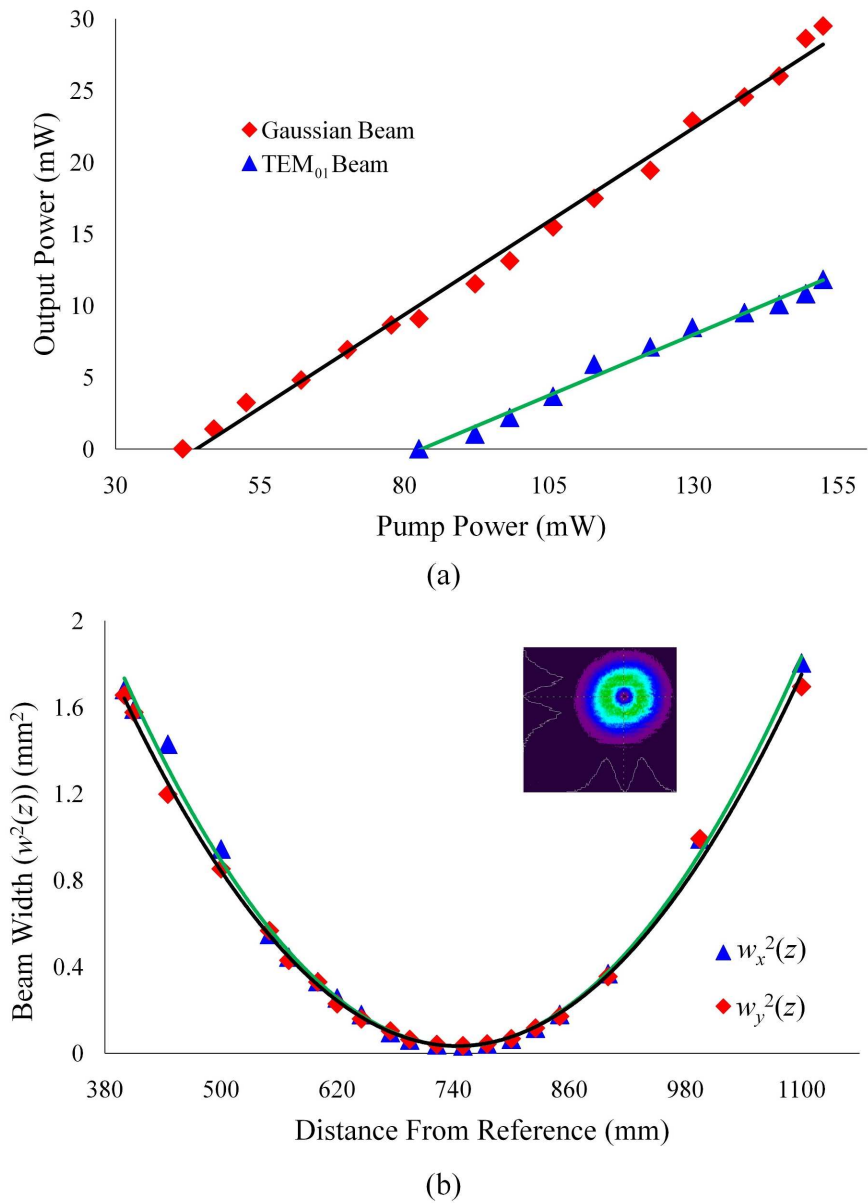
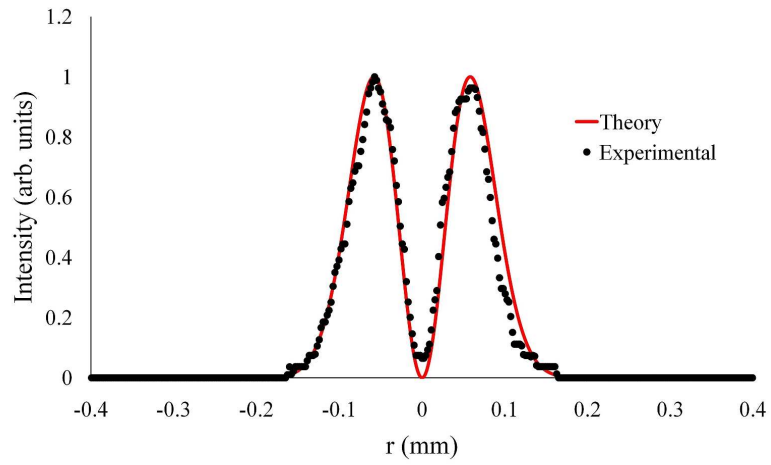
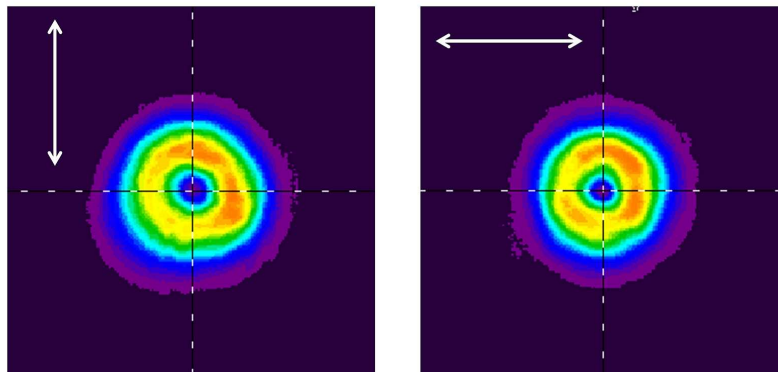


Figure 4: (a) Slope efficiencies of a Gaussian and LG₀₁ output with the Gaussian and donut shaped pump profiles respectively; (b) Free space propagation of the LG₀₁ beam (in the two principal axes) from which the beam quality factor (M^2) could be inferred (and similarly for the Gaussian beam). The inset in (b) shows the far-field image of the LG₀₁ eigenmode.



(a)



(b)

(c)

Figure 5: (a) Comparison of the intensity profiles calculated LG_{01} mode at the output coupler and the measured intensity, showing good agreement. The intensity is invariant under rotation of polarisation: (b) after passing through a vertically aligned polariser and (c) a horizontally aligned polariser.

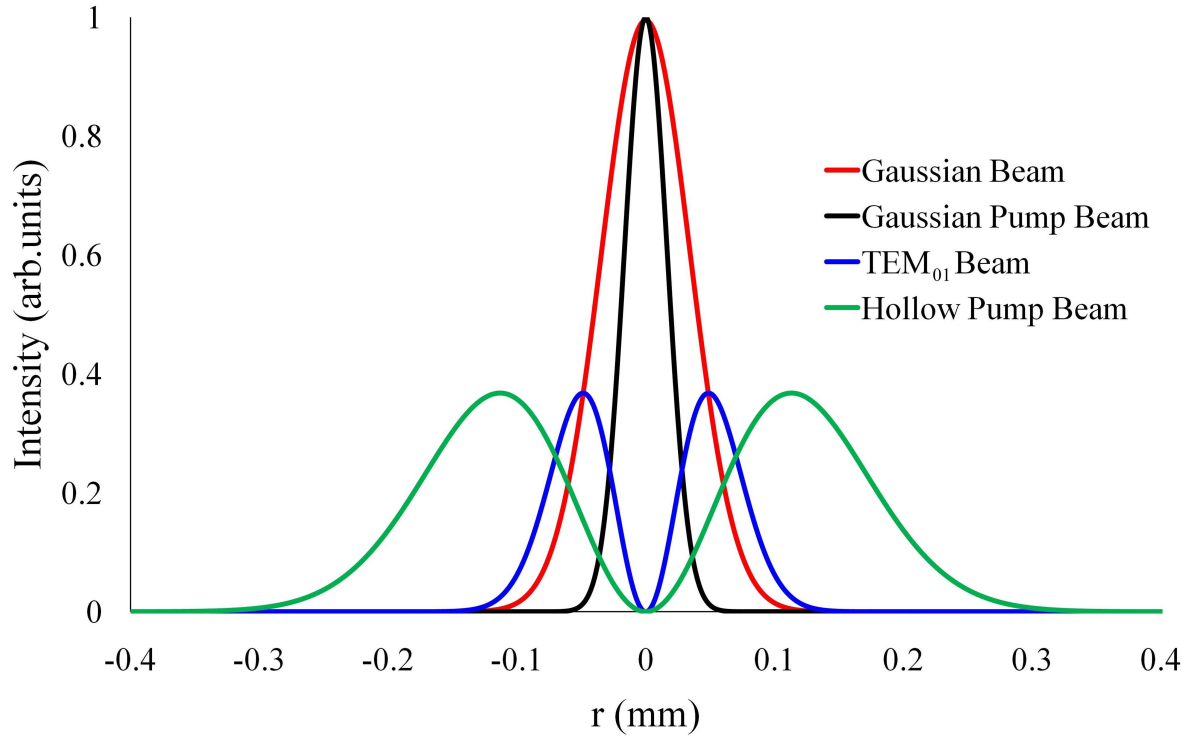


Figure 6: Intensity profiles of the Gaussian and LG_{01} modes for the correspondingly shaped pump beam, for the $f = 100$ mm case. The overlap between the modes, and well as the distribution of energy, is evident.